

Small-conductance Cl⁻ channels contribute to volume regulation and phagocytosis in microglia

Guillaume Ducharme,^{1,2} Evan W. Newell,^{1,2} Crystal Pinto¹ and Lyanne C. Schlichter^{1,2}

¹Toronto Western Research Institute, University Health Network, University of Toronto, Toronto, Ontario, Canada M5T 2S8

²Department of Physiology, University of Toronto, Toronto, Ontario, Canada M5S 1A8

Keywords: anion channel expression, biophysical properties, noise analysis, rat, regulatory volume decrease, swelling-activated channels

Abstract

The shape and volume of microglia (brain immune cells) change when they activate during brain inflammation and become migratory and phagocytic. Swollen rat microglia express a large Cl⁻ current ($I_{Cl_{swell}}$), whose biophysical properties and functional roles are poorly understood and whose molecular identity is unknown. We constructed a fingerprint of useful biophysical properties for comparison with $I_{Cl_{swell}}$ in other cell types and with cloned Cl⁻ channels. The microglial $I_{Cl_{swell}}$ was rapidly activated by cell swelling but not by voltage, and showed no time-dependence during voltage-clamp steps. Like $I_{Cl_{swell}}$ in many cell types, the halide selectivity sequence was $I^- > Br^- > Cl^- > F^-$. However, it differed in lacking inactivation, even at +100 mV with high extracellular Mg²⁺, and in having a much lower single-channel conductance: 1–3 pS. Based on these fundamental differences, the microglia channel is apparently a different gene product than the more common intermediate-conductance $I_{Cl_{swell}}$. Microglia express several candidate genes, with relative mRNA expression levels of: CLIC1 > CIC3 > $I_{Cl_{in}} \geq CIC2 > Best2 > Best1 \geq Best3 > Best4$. Using a pharmacological toolbox, we show that all drugs that reduced the microglia current (NPPB, IAA-94, flufenamic acid and DIOA) increased the resting cell volume in isotonic solution and inhibited the regulatory volume decrease that followed cell swelling in hypotonic solution. Both channel blockers tested (NPPB and flufenamic acid) dose-dependently inhibited microglia phagocytosis of *E. coli* bacteria. Because $I_{Cl_{swell}}$ is involved in microglia functions that involve shape and volume changes, it is potentially important for controlling their ability to migrate to damage sites and phagocytose dead cells and debris.

Introduction

Patch-clamp studies have revealed the nearly ubiquitous presence of a swelling-activated chloride current, $I_{Cl_{swell}}$. Owing to its activation following exposure of cells to a hypotonic solution, the main function conjectured for $I_{Cl_{swell}}$ is regulatory volume decrease (RVD). RVD involves coordinated activation of $I_{Cl_{swell}}$ and a K⁺ channel(s), resulting in electroneutral KCl extrusion and passive water loss to restore cell volume (Roman *et al.*, 1996; Mignen *et al.*, 1999; Jentsch *et al.*, 2002; d'Anglemon de Tassigny *et al.*, 2003; Nilius & Droogmans, 2003; Sardini *et al.*, 2003). Pharmacological studies support roles for $I_{Cl_{swell}}$ in proliferation (Schumacher *et al.*, 1995; Shen *et al.*, 2000; Wondergem *et al.*, 2001), migration (Ransom *et al.*, 2001; Kim *et al.*, 2004) and apoptosis (Okada *et al.*, 2006). Several molecular candidates have been proposed as the volume-regulated anion channel (VRAC), with none gaining general acceptance. To help identify the endogenous channels, biophysical and pharmacological fingerprints are often constructed. $I_{Cl_{swell}}$ have some general similarities in different cells, i.e. lack of voltage- and time-dependent activation, a requirement for intracellular ATP or a nonhydrolysable analogue, a broad permeability to anions (following Isenman sequence I, i.e. $I^- \geq Br^- \geq Cl^-$) and mild outward rectification in

symmetrical Cl⁻ solutions. However, conflicting single-channel conductance values have been reported, from very small to intermediate outwardly rectifying (Jentsch *et al.*, 2002; Nilius *et al.*, 2003). Moreover, the degree of channel inactivation is highly variable and appears to depend on the cell type (Jentsch *et al.*, 2002). Such differences might indicate heterogeneity in the molecular determinants. Two key problems in identifying heterologously expressed Cl⁻ channels are the nearly ubiquitous expression of endogenous Cl⁻ channels and the possible expression of multiple $I_{Cl_{swell}}$ channels with some overlapping properties.

Microglia, the resident immune cells of the brain, possess a complex array of ion channels, including a swelling-sensitive Cl⁻ channel that contributes to the membrane potential (Newell & Schlichter, 2005) and to proliferation (Schlichter *et al.*, 1996) of rat microglia. A similar current in cultured murine microglia apparently helps maintain their ramified morphology (Eder *et al.*, 1998), and supports chemokine-induced migration (Rappert *et al.*, 2002). Although the same current is assumed to mediate volume regulation in microglia, this has never been tested and, because many properties of $I_{Cl_{swell}}$ in microglia are unknown, limited comparisons could be made with previously described and cloned chloride channels. Furthermore, among the candidate genes proposed for $I_{Cl_{swell}}$, it is not known which are expressed in microglia. The present study was designed to fill several of these crucial knowledge gaps and to assess roles of this current in important microglia functions. First, we assessed several key properties of the current in order to facilitate

Correspondence: Dr Lyanne C. Schlichter, MC9-417, Toronto Western Hospital, 399 Bathurst Street, Toronto, Ontario, Canada M5T 2S8.
E-mail: schlicht@uhnres.utoronto.ca

Received 08 June 2007, revised 23 July 2007, accepted 01 August 2007

comparisons with other cell types and cloned Cl^- channels. Then, we quantitatively compared transcript expression of several Cl^- channel genes that might underlie the current. Finally, we not only linked the microglial current to its classical function, regulatory volume decrease, but showed for the first time that it contributes to homeostatic volume regulation and to the essential microglia function of phagocytosis.

Materials and methods

Cell cultures

Microglia were isolated from brains of 2- to 3-day-old Wistar rats, as previously described (Fordyce *et al.*, 2005; Newell *et al.*, 2005; Kaushal *et al.*, 2007). Rat pups were killed by cervical dislocation in accordance with guidelines from the Canadian Institutes of Health Research and the University Health Network. After carefully removing the meninges, whole brain tissue was mashed through a stainless steel sieve (100 mesh; Tissue Grinder Kit no. CD-1; Sigma), and then pelleted, re-suspended and seeded into flasks with Minimal Essential Medium containing 5% fetal bovine serum, 5% horse serum and 100 μM gentamycin (all from Invitrogen). Two days later, cellular debris, nonadherent cells and supernatant were removed and fresh medium was added to the flask. The mixed cultures were allowed to grow for 7–10 days and then shaken for 4 h on an orbital shaker at 8–10 Hz in a standard tissue culture incubator. The supernatant containing detached microglia was centrifuged and the cell pellet was resuspended for counting, and then plated according to the particular experiment. Microglia were plated at 3.5×10^4 cells per 15-mm-diameter glass coverslip for electrophysiology, and at 5.0×10^4 cells per well in 96-well (black-walled) plates (Corning, Acton, MA, USA) for the phagocytosis assay. Before experiments, the plated microglia were cultured for 1–3 days in Minimal Essential Medium with 100 μM gentamycin and a reduced serum concentration (2% fetal bovine serum) to decrease their spontaneous activation. This procedure yielded highly purified cultures of microglia (99–100%; see Fig. 4), as judged by labelling with FITC-conjugated isolectin B4 or tomato lectin (Sigma), or by immunofluorescence using the OX-42 monoclonal antibody (Serotec, Raleigh, NC, USA), which recognizes complement receptor 3. In addition, we previously demonstrated nearly 100% purity with quantitative real-time reverse transcriptase–polymerase chain reaction (qRT-PCR; Kaushal *et al.*, 2007). From this unstimulated state, a variety of treatments can activate the microglia: activating NF- κB and p38 MAPK signalling pathways; up-regulating iNOS and production of reactive oxygen and nitrogen species; and causing them to kill healthy neurons (Fordyce *et al.*, 2005; Kaushal *et al.*, 2007).

Patch-clamp electrophysiology

Recordings were made in the whole-cell configuration with 4–5 $\text{M}\Omega$ -resistance pipettes pulled from thin-wall borosilicate glass capillaries (WPI, Sarasota, FL, USA). Currents were recorded with an Axopatch 200 integrating patch-clamp amplifier (Axon Instruments, Molecular Devices, Sunnyvale, CA, USA), digitized with a DigiData 1200 board, and acquired and analysed with pCLAMP version 8.0 software (Axon Instruments). The currents were filtered online using the low-pass Bessel filter of the amplifier at 5 kHz, except for noise analysis, when 10 kHz was used.

Whole-cell recordings were established with the standard bath solution, containing (in mM): NaCl, 125; KCl, 5; CaCl_2 , 1; MgCl_2 , 1; and HEPES, 10 (pH 7.4, 300 mOsm). Then, to minimize cation currents (e.g. the prevalent K^+ currents) and isolate $\text{I}_{\text{Clswell}}$, the bath

was changed to a Na^+ - and K^+ -free *N*-methyl-D-glucamine (NMDG⁺) solution (in mM: NMDG-Cl, 140; CaCl_2 , 1; MgCl_2 , 1; and HEPES, 10; pH 7.4, 300 mOsm). The pipette contained an NMDG⁺ solution (in mM): NMDG-Cl, 50; NMDG-aspartate, 70; CaCl_2 , 1; MgCl_2 , 1; HEPES, 10; EGTA, 10; and MgATP, 2 (pH 7.2, 300 mOsm), with low free Ca^{2+} (~ 20 nM). The osmolarity of each solution was measured with a freezing-point depression osmometer and adjusted by adding sucrose, if necessary. $\text{I}_{\text{Clswell}}$ was activated by applying a hypotonic solution (having 55% of the normal osmolarity, i.e. 165 mOsm) made with a 1 : 1 v/v dilution of the NMDG⁺ bath and a solution containing only (in mM): CaCl_2 , 1; MgCl_2 , 1; and NMDG-HEPES, 10 (pH 7.4, 30 mOsm). For one type of experiment, a low-ionic-strength pipette solution was used in which the NMDG-aspartate was omitted and the osmolarity was adjusted with extra sucrose. Unless otherwise indicated, all chemicals were from Sigma-Aldrich (Oakville, ON, Canada).

Microglia on coverslips were rinsed with standard bath solution and mounted in the recording chamber, and recordings were made at room temperature. The junction potential between the bath and pipette solution before seal formation was -2 mV, and this value was not subtracted from the data in the figures. For most experiments (except for ionic selectivity; see below), the agar bridge was made with NaCl bath solution. This did not affect the junction potential when bath solutions were changed, except for the NMDG bath solution, for which the additional -4 mV junction potential was corrected in all recordings. For specific experiments, we used five classical Cl^- channel blockers: the disulphonic stilbenes, 4,4'-diisothiocyanatostilbene-2,2'-disulphonic acid (DIDS) and 4-acetamido-4'-isothiocyanatostilbene-2,2'-disulphonic acid (SITS); the indanylalkanoic acid IAA-94; and the fenamates, 5-nitro-2-(3-phenylpropylamino) benzoic acid (NPPB) and flufenamic acid (FFA; Sigma). We also tested an inhibitor of the I_{Clm} chloride channel, acyclovir (Furst *et al.*, 2000), an inhibitor of the Na^+ - K^+ - Cl^- symporter, bumetanide, and an inhibitor of the K^+ - Cl^- cotransporter, [(dihydroindanyl)oxy]acetic acid (DIOA; Sigma).

To calculate the relative anion permeability of $\text{I}_{\text{Clswell}}$, the current was activated with the 55% hypotonic solution and the amplitude was allowed to stabilize, after which the Cl^- bath solution was exchanged for a similarly hypotonic solution with the test anion (Γ^- , Br^- , F^- , aspartate or glutamate). The change in reversal potential (ΔE_{rev}) between the two solutions was measured and the relative permeability was calculated using a modified version of the Goldman–Hodgkin–Katz equation.

$$P_{\text{A}^-/\text{Cl}^-} = \left\{ [\text{Cl}_0^-]_{\text{before}} \exp(\Delta E_{\text{rev}} z F / RT) - [\text{Cl}_0^-]_{\text{after}} \right\} / [\text{A}_0^-]_{\text{after}} \quad (1)$$

where $[\text{Cl}_0^-]_{\text{before}}$ is the initial 74 mM Cl^- concentration, $[\text{Cl}_0^-]_{\text{after}}$ is the 4 mM Cl^- concentration remaining after changing the external anion, $[\text{A}_0^-]_{\text{after}}$ is the concentration of the test anion after the solution change and z is the valence. For each anion, several cells were tested and the permeability ratios were calculated and averaged. Importantly, for these experiments, a 3 M KCl agar bridge was used to prevent junction potential changes when the anion species was changed in the bath.

qRT-PCR

Transcript levels were monitored by qRT-PCR, as previously described (Bustin & Nolan, 2004; Kaushal *et al.*, 2007). Gene-specific primers (Table 1) were designed using the 'Primer3Output' program (http://frodo.wi.mit.edu/cgi-bin/primer3/primer3_www.cgi). RNeasy mini kits (Qiagen) were used to isolate RNA after degrading any contaminating DNA with DNaseI (0.1 U/mL, 15 min, 37 °C;

TABLE 1. Sequences of primers used for quantitative RT-PCR analysis

Primer	Accession number	Sequence
HPRT-1*	NM_012583.2	F: CAGTACAGCCCCAAAATGGT R: CAAGGGCATATCCAACAACA
CIC-2	X64139	F: CCACCTTCTTCGCTGTAGG R: TTCTTCATCACGGTTCCACA
CIC-3	XM_341428	F: AGTGGAAAACATGGGCAGAG R: GCAAAACTCAAAGCCCAAAA
CLIC1	XM_345083	F: GCTCCCGTTCTGCTCTA R: CGGGTTTGAGTTCTTGATGTAG
I _{Clswell}	NM_031719	F: AGGCGTCCGAACAGAAGA R: CTGCTGGTGACAGCTTGC
Best1	NM_001011940.1	F: GTGGCAGAACAGCTCATCAA R: CATCCATCCACAGACAACA
Best2	XM_344742.3	F: ACCCACTCCCTAGCATCTT R: CCACTGGAAGGGAAGAACAC
Best3	XM_001066317.1	F: AGCGTATTTATGCCAGGTG R: GGCAGTGGAAATGTGTGTA
Kv1.3	M30312	F: GCTCTCCGCCATTCTAAG R: TCGTCTGCCTCAGCAAAGT

*Housekeeping.

Amersham Biosciences). A two-step reaction was performed according to the manufacturer's instructions (Invitrogen); i.e. total RNA (1 µg) was reverse-transcribed in a 20-µL volume using 200 U of SuperScriptII RNase H-reverse transcriptase, with 0.5 mM dNTPs (Invitrogen) and 0.5 µM oligo dT (Sigma). Amplification was performed on an ABI PRISM 7700 Sequence Detection System (PE Biosystems, Foster City, CA, USA) at 95 °C for 10 min, followed by 40 cycles at 95 °C for 15 s, 56 °C for 15 s and 72 °C for 30 s, 'No-template' and 'no-amplification' controls were included for each gene, and melt curves showed a single peak, confirming specific amplification (Bustin *et al.*, 2004). The threshold cycle (C_T) for each gene was determined and normalized against the housekeeping gene hypoxanthine guanine phosphoribosyl transferase (HPRT-1).

Monitoring volume regulation by flow cytometry

To examine the contribution of I_{Clswell} to regulating microglia volume, we measured forward light scatter using flow cytometry, as widely used (Downey *et al.*, 1995; Ormerod *et al.*, 1995; Khanna *et al.*, 1999). For these experiments, microglia were harvested from the supernatants of flasks immediately after shaking for 4–8 h at 37 °C in the incubator. After harvesting the cells, they were suspended in the standard bath solution (same as for patch clamping) in the absence or presence of inhibitors of the Cl⁻ channels or transporters (see above). For each condition and time-point, three replicate tubes containing microglia were sampled. After ~10 min incubation with each inhibitor, a baseline reading was taken for each condition. The 30 mOsm dilution buffer (see above) was then added to each of the remaining samples (final osmolarity ~55% of normal; ~165 mOsm). Thus, because a 55% hypotonic dilution solution caused a reproducible swelling and a small but readily detectable RVD without cell death, it was used for subsequent experiments. The remaining samples were run in triplicate at specific times after exposure to the hypotonic solution. Experiments were conducted entirely at room temperature or the cells were maintained at 37 °C by keeping the tubes in a water bath until used. For each statistical replicate, volume regulation assays were performed on a batch of cells prepared from a different rat litter. Because the forward scatter values obtained by the flow

cytometer are arbitrary, for each replicate they were normalized to untreated cells in the standard bath solution.

Phagocytosis assay

Microglia phagocytosis of bacteria (*E. coli*, labelled with FITC) was assessed using the Vybrant Phagocytosis Assay Kit according to the manufacturer's instructions (V-6694; Molecular Probes). In brief, fluorescent *E. coli* in suspension were added to each test well for 1 h, with or without a chloride channel blocker: NPPB or FFA. The *E. coli* suspension was then removed by vacuum aspiration, followed immediately by a 1-min treatment with trypan blue to quench the fluorescence of any *E. coli* adhering to the outside of the microglia. The total fluorescence of each well was then measured using a fluorescence plate reader (SPECTRAMax Gemini EM; Molecular Devices) at 480 nm excitation and 520 nm emission wavelengths. Each treatment was run in triplicate on the same plate and averaged to yield a single statistical replicate (n). For statistical comparisons, experiments were repeated on cells isolated from different rat litters. Phagocytosis indices were normalized to the solvent control (0.2% DMSO), which was the highest concentration used. The solvent control and untreated cells did not differ ($P = 0.50$, one-sample t -test).

Statistics

All statistics (Student's t -tests and ANOVA) and curve fitting were conducted using Origin ver7.0 software (OriginLab, Northampton, MA, USA). To test for significant differences between anion permeabilities, and between relative mRNA levels, one-way ANOVAs were used, followed by Tukey's test for multiple comparisons.

Results

Hypotonic shock activated a Cl⁻ conductance

To investigate Cl⁻ currents in rat microglia, both Na⁺ and K⁺ from the standard bath and pipette solutions were replaced with the bulky cation NMDG⁺. This eliminated several cation currents that are characteristic of microglia (Kv1.3, Kir2.1 and TRPM7), leaving an extremely small remaining current when the solutions were isotonic and external Cl⁻ was 144 mM (Fig. 1A and B, trace 1). Then, when the hypotonic solution was perfused into the bath (55% normal osmolarity), a large current developed over the next couple of minutes; this current was outwardly rectifying despite similar internal (54 mM) and external (74 mM) Cl⁻ concentrations. The volume sensitivity was further demonstrated by its decrease when the original isotonic solution was restored. These properties are entirely consistent with our initial description of this current in rat microglia (Schlichter *et al.*, 1996). We also found that a 20% hypotonic solution activated the current, but more slowly and with a much more variable amplitude (not shown). The Cl⁻ current activated spontaneously when a low ionic strength pipette solution was used (Fig. 1C). In this case, the current activated rapidly after break-in, reached a peak by ~5 min and then spontaneously ran down by ~25 min. Its subsequent volume sensitivity was confirmed by applying a hypertonic NMDG bath solution (350 mOsm), after which the current declined very rapidly. For the remainder of this study, we used the 55% hypotonic bath solution to activate the current because it produced a rapid response with a sufficiently stable plateau phase for testing treatments. Nevertheless, the

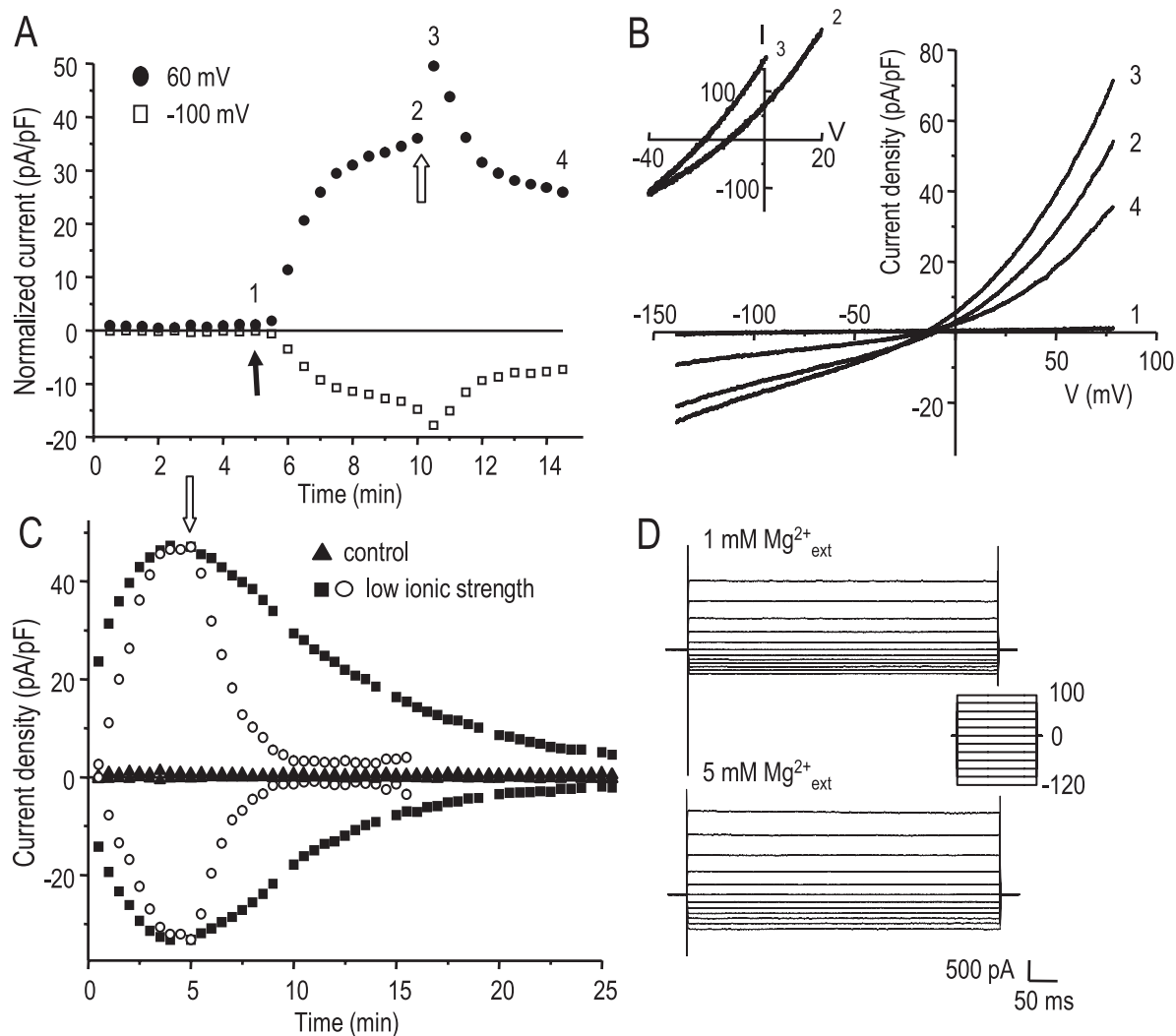


FIG. 1. Activation of an osmosensitive Cl^- current, I_{Clswell} , in primary rat microglia. (A) Representative whole-cell currents recorded in Na^+ - and K^+ -free solutions at +60 and -100 mV. After a 55% hypotonic bath solution was perfused in (closed arrow), a large current developed; this was then reduced after a slightly hypertonic bath solution (350 mOsm) was applied (open arrow). The transient increase after the open arrow is explained in the text. (B) Current-vs-voltage relationships measured at the time points indicated in panel A. Note the very small background current under isotonic conditions (trace 1), activation of an outwardly rectifying current by 55% hypotonic solution (74 mM Cl^- , trace 2) and increase in the current immediately after the external Cl^- concentration was increased (trace 3), i.e. after a hypertonic (~ 350 mOsm) NMDG bathing solution with 144 mM Cl^- was perfused in. The expanded traces (inset) show the shift in reversal potential when external Cl^- was changed from 74 to 144 mM, providing evidence for its Cl^- dependence. (C) Spontaneous activation of the current by low intracellular ionic strength. The pipette solution had the same Cl^- concentration (54 mM), but the 70 mM NMDG-aspartate was replaced with sufficient sucrose to balance the osmolarity. Under these conditions, with the normal osmolarity bath solution (\blacktriangle), the Cl^- current developed and then ran down spontaneously. This current was more rapidly inhibited if a hypertonic bath solution (350 mOsm; open arrow) was perfused in (\circ). When both the osmolarity and ionic strength of the pipette solution were normal (\blacktriangle), only a small background current was present. (D) Lack of voltage-dependent inactivation with either 1 or 5 mM extracellular Mg^{2+} . Traces show a family of whole-cell currents at the time of maximal activation after applying the 55% hypotonic solution. Voltage steps were applied between -120 and $+100$ mV, from a holding potential of 0 mV.

amplitude was highly variable; i.e. after 5 min in this solution the mean current was 886 ± 561 pA (current density 42 ± 26 pA/pF; mean \pm SD; $n = 11$). Of note, the amplitude did not simply correlate with cell size as measured by the whole-cell capacitance ($R^2 = 0.13$; $P > 0.2$; $n = 11$). Its identity as a Cl^- current was confirmed (Fig. 1B, inset) by a reversal potential (-12 mV) close to the Cl^- Nernst potential (-10 mV), and a shift to -21 mV when the external Cl^- concentration was increased from 74 to 144 mM (Nernst potential, -25 mV). All reversal potentials were calculated using the chloride activity coefficient. Note also the brief increase in current resulting from the increase in external Cl^- . This was thus a

swelling-activated Cl^- current, and the next question was whether it was the same as I_{Clswell} in other cell types.

Biophysical properties of I_{Clswell} in microglia

To assess whether the microglial I_{Clswell} is likely to be the same molecular entity as in other cell types, it is useful to compare biophysical properties that are most likely to arise from the protein sequence and contribute to a molecular fingerprint. I_{Clswell} in most cells inactivates at depolarized potentials (usually above $+40$ mV),

and one cloned channel (ClC-2) shows voltage-dependent activation at hyperpolarized potentials (see Discussion). We found that the microglial whole-cell current had a current–voltage relation that was outwardly rectified but did not show voltage-dependent or time-dependent activation or inactivation (Fig. 1D). Because the degree of inactivation in some cells is affected by extracellular Mg²⁺, we supplemented the hypotonic bath solution with 4 mM MgCl₂ (total Mg²⁺, 5 mM) after I_{Clswell} had reached its maximal amplitude (Fig. 1D). The elevated Mg²⁺ did not confer inactivation, even at +100 mV; thus, the microglial current apparently lacked voltage-dependent inactivation, and in this way differed from I_{Clswell} in many other cells.

Cl⁻ channel selectivity among halide ions is a useful biophysical fingerprint, but has not been reported for the microglial current. We determined the channel's relative permeability to different anions under bi-ionic conditions when external Cl⁻ was replaced with a test anion after I_{Clswell} had reached its maximal amplitude (Fig. 2). Using a modified Goldman–Hodgkin–Katz equation (see Eqn 1 in Materials and methods), the permeability of each test anion vs. chloride was calculated by measuring changes in reversal potential and averaged. The permeability sequence was $\Gamma = \text{Br}^- > \text{Cl}^- > \text{F}^- > \text{aspartate} \geq \text{glutamate}$, where '>' denotes a significant difference ($P < 0.05$) and '≥' indicates a trend that did not reach statistical significance. This halide permeability sequence corresponds with Eisenman's sequence I, and is similar to I_{Clswell} in many other cell types.

The single-channel conductance is another basic biophysical parameter that can be used to help identify a channel; hence this feature of I_{Clswell} has been examined in several cell types. We employed two complementary approaches based on stationary noise analysis. In traditional noise analysis, the simplest approach is to assume that the number of active channels remains constant, such that current activation is due to a graded increase in channel open probability (P_o). If so, the variance and mean current can be measured while the current runs up, and the single-channel current can be determined from the mean current–vs.–variance plot fitted to Eqn 2.

$$\sigma^2 = iI - I^2/N \quad (2)$$

where σ^2 is the measured variance of the whole cell current (I), N is the number of channels and i is the unitary current. First, we used this approach for the whole-cell Cl⁻ current activated when microglia were exposed to a 55% hypotonic bath solution. During I_{Clswell} run-up the membrane potential was repeatedly stepped (every 5 s) from 0 to 50 mV for 400 ms, and the mean current and variance during each step were measured (Fig. 3). The calculated single-channel current was 0.043 ± 0.010 pA, corresponding to a single-channel conductance of 0.72 ± 0.17 pS (mean \pm SD; $n = 7$). An assumption is that the current is stationary, and the small run-up during each 400-ms-long step would produce a slight over-estimate of the variance and single-channel conductance.

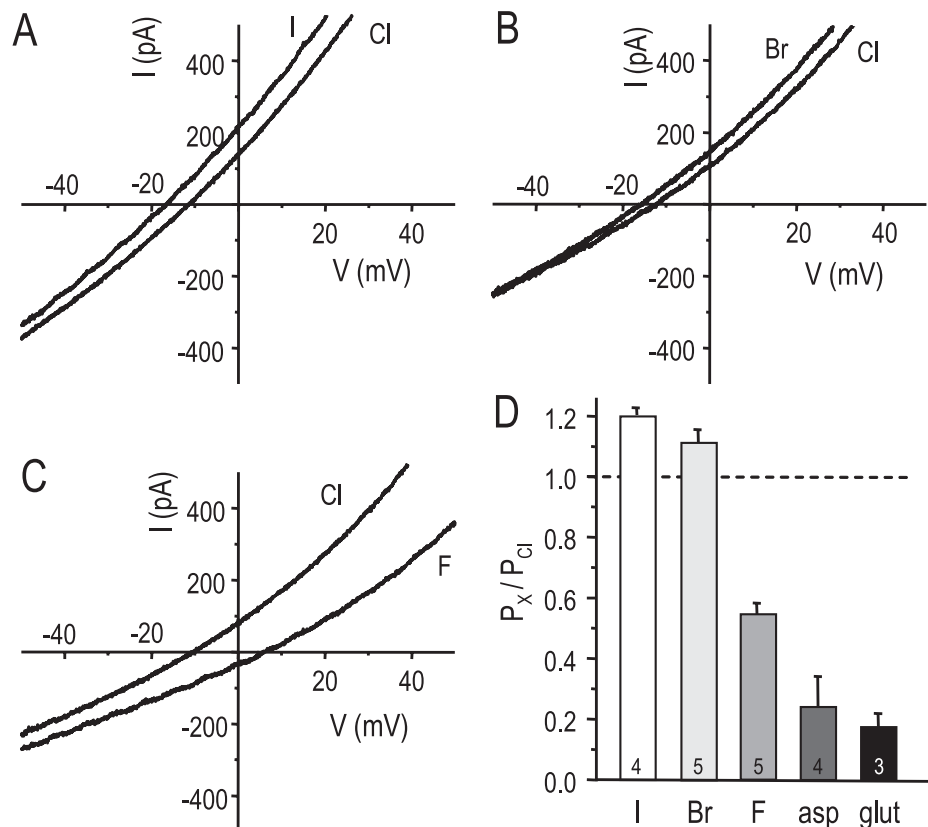


FIG. 2. Anion selectivity of the swelling-activated Cl⁻ current. (A–C) Representative traces showing the change in reversal potential when extracellular Cl⁻ was replaced by Γ , Br⁻ or F⁻. (D) Summary of anion permeability relative to Cl⁻ (mean \pm SD; n indicated on each bar), calculated using a modified version of the Goldman–Hodgkin–Katz equation (see Eqn 1 in Materials and methods). The change in reversal potential was measured when Cl⁻ in the extracellular solution was replaced with the test anion. All pair-wise comparisons were statistically significant (one-way ANOVA, followed by Tukey's test; $P < 0.05$) except Γ vs. Br⁻ and aspartate vs. glutamate.

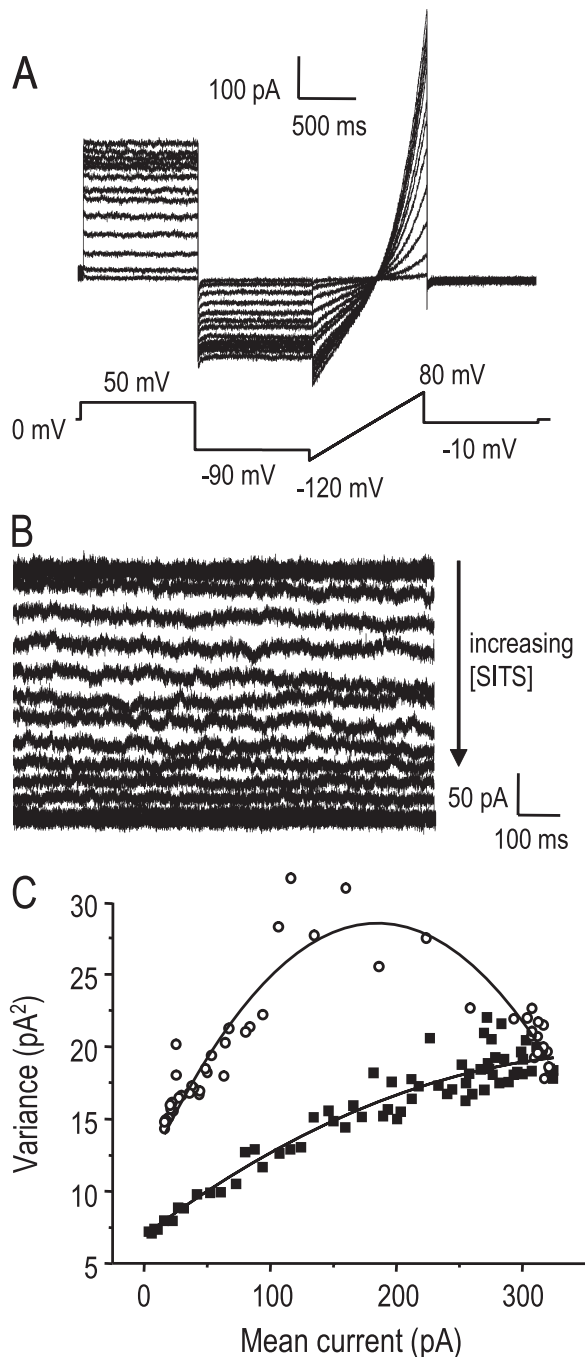


FIG. 3. Single-channel conductance from noise analysis of $I_{Clswell}$. (A) A representative recording beginning immediately after the 55% hypotonic solution was perfused into the bath. Run-up of $I_{Clswell}$ is seen during repeated voltage-clamp steps to +50 mV and then to -90 mV, followed by a ramp from -120 to +80 mV from a holding potential of 0 mV. This protocol was run every 5 s until the current reach its maximum amplitude; some traces have been omitted for clarity. For stationary noise analysis, the mean current and variance was calculated during each step to +50 mV. (B) In the same cell, an alternative method was used for stationary noise analysis. After $I_{Clswell}$ had reached a plateau, the current was monitored at +50 mV as it was progressively blocked by a slowly increasing concentration of the Cl^- channel blocker SITS (arrow). The mean current and variance were calculated from such records after correcting for baseline drift. (C) Mean-vs.-variance plots comparing the two methods on the same cell. Each data set (from panels A and B) was fitted to Eqn 2 (see Results). For this cell, the single-channel conductance was calculated as 1.10 pS during $I_{Clswell}$ run-up (■) and 3.15 pS from the SITS titration protocol (○).

It was important to compare this analysis with another approach because the assumption that current run-up represents a graded increase in open probability appears to be invalid for $I_{Clswell}$ in some cells (Jackson & Strange, 1995b; Boese *et al.*, 1996). In those studies, it was possible to also perform nonstationary noise analysis during the pronounced voltage-dependent inactivation of $I_{Clswell}$ at highly positive potentials, and to compare results with stationary noise analysis done on current run-up. Their analysis showed unambiguously that run-up involves an increase in the number of active channels and that the single-channel conductance in C6 glioma cells is intermediate, with outward rectification (Jackson *et al.*, 1995b). The same approach was not possible in the present study, because $I_{Clswell}$ in microglia lacks voltage-dependent inactivation. In this, the microglia current is much like the current in T lymphocytes, which also did not inactivate and had an apparent single-channel conductance < 1 pS (Schumacher *et al.*, 1995).

In our second approach, we used a chloride channel blocker (SITS). The main assumption was that an increase in blocker concentration reduces the $I_{Clswell}$ amplitude by reducing the open probability. The blocker should have intermediate on-off rates; if the dissociation rate is too slow, the 'apparent' number of active channels will decrease and, if too fast, the 'apparent' single-channel conductance will decrease. If this assumption is met and the blocker concentration is increased slowly enough, the resulting current will be quasi-stationary for short time periods, allowing calculation of the single-channel conductance from the resulting mean-vs.-variance plot. To implement this approach, $I_{Clswell}$ was first activated and stationary noise analysis performed on the current run-up (as above), and then a solution containing 2 mM SITS was added stepwise ($\sim 10 \mu\text{L}/\text{pulse}$ added to the $\sim 400 \mu\text{L}$ bath) to gradually increase its concentration (Fig. 3B). Because SITS exhibited time- and depolarization-dependent block (Lewis *et al.*, 1993; Nilius *et al.*, 2003; present study), the membrane potential was continuously held at +50 mV to obtain a quasi-stationary record. Thus, as the drug concentration increased, the block remained near equilibrium. The mean current-vs.-variance plot of each record was constructed and compared with the stationary noise analysis from current run-up in the same cell (Fig. 3C). From the SITS titration method, the calculated single-channel conductance was 3.54 ± 1.31 pS (mean \pm SD; $n = 3$); that is, it remained low but was significantly higher than from noise analysis during current run-up ($P < 0.001$, two-sample *t*-test). Because of this difference, we verified that the filtering bandwidth and duration of sampling were appropriate for measuring the SITS-induced variance, as follows. For the data above, we used a 20-kHz sampling rate and a 10-kHz low-pass filter, and the variance was sampled for periods of 1000 ms each as the SITS concentration slowly increased. Importantly, we found that the calculated single-channel conductance was not affected by decreasing the filter cutoff to 3000, 1000 or 500 Hz, or reducing the sampling period to 750 or 500 ms. Thus, even the higher concentrations of SITS appeared to change the probability of opening, rather than the ability to resolve single-channel currents. Lower frequencies or shorter durations decreased the apparent single-channel conductance, by $\sim 40\%$ at 10 Hz and $\sim 50\%$ at 100 ms.

Expression of putative $I_{Clswell}$ genes

With this biophysical fingerprint in hand, we next monitored the relative expression of genes that have been proposed to underlie swelling-activated Cl^- currents. qRT-PCR was used to compare mRNA expression levels in cultures of microglia that were shown to be essentially 100% pure (Fig. 4), after normalizing to the house-keeping gene, HPRT-1. Several known or putative Cl^- channel genes

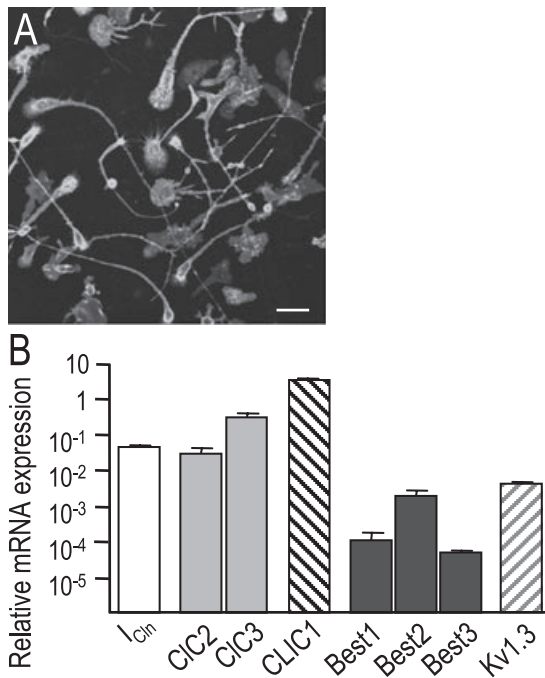


FIG. 4. Expression of putative swelling-activated Cl⁻ channel genes. (A) Demonstration of culture purity, showing that 100% of the cells in a representative microglia culture labeled with the microglia-specific marker, tomato lectin, conjugated to FITC. (B) Relative mRNA expression was monitored by qRT-PCR, normalized to the housekeeping gene HPRT-1 (see Materials and methods). Values shown are mean \pm SD from four separate batches of microglia isolated from different rat litters. Scale bar, 25 μ m.

were detected, with the following order of mRNA expression: CLIC1 > CIC3 > I_{ClIn} \geq CIC2 > Best2 > Best1 \geq Best3 > Best4. For comparisons of transcript levels, '>' denotes a significant difference ($P < 0.05$) and ' \geq ' indicates a trend that did not reach statistical significance. The potassium channel, Kv1.3, was included because it is a key candidate for the K⁺ component of the K⁺, Cl⁻ and water loss during RVD. Kv1.3 is also a useful comparator as we can estimate the number of active Kv1.3 channels from our previous studies as 500–1000/cell, calculated by dividing the whole-cell Kv1.3 conductance (5–10 nS; Newell *et al.*, 2005) by the single-channel Kv1.3 conductance (~ 10 pS; Pahapill & Schlichter, 1992). Several of the genes were expressed at higher levels than Kv1.3 (CLIC1, I_{ClIn}, CIC-2, CIC-3) and CLIC1 expression was higher than that of the housekeeping gene HPRT-1.

I_{ClSwell} contributed to volume regulation in microglia

Because there are no potent, selective blockers of I_{ClSwell}, the first step was to identify compounds for use in the functional assays (Fig. 5). We tested three classical Cl⁻ channel blockers (IAA-94, NPPB and FFA), and inhibitors of I_{ClIn} (acyclovir; Furst *et al.*, 2000), the Na⁺-K⁺-Cl⁻ symporter (bumetanide) and the K⁺-Cl⁻ cotransporter (DIOA). For each drug, the concentration was chosen to produce >50% inhibition of their respective targets. Effects of each drug on I_{ClSwell} were determined at -50 mV, the approximate resting membrane potential of cultured microglia (Newell *et al.*, 2005). For NPPB, IAA-94 and FFA, the predicted extent of I_{ClSwell} block was $\geq 70\%$ at the concentrations tested (Schumacher *et al.*, 1995; Schlichter *et al.*, 1996), and we observed nearly complete block of I_{ClSwell} by 150 μ M NPPB and 300 μ M FFA, and $\sim 70\%$ block by 500 μ M IAA-94

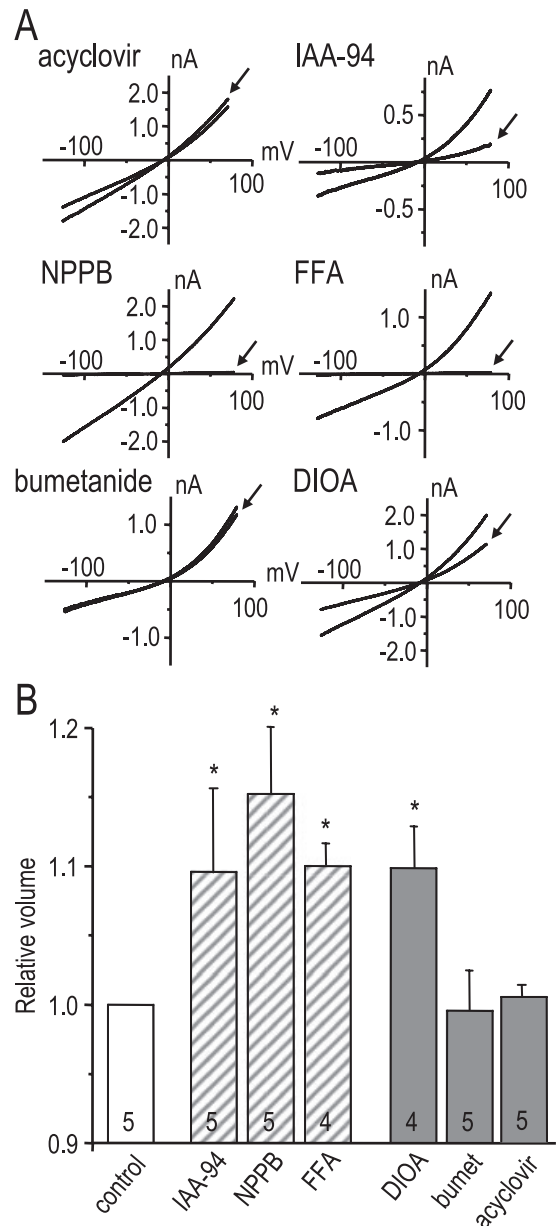


FIG. 5. Blockers of I_{ClSwell} inhibited homeostatic volume regulation. (A) Representative whole-cell current traces in response to voltage ramps during the plateau phase of the swelling-activated current, I_{ClSwell}, to show effects of each compound used to study microglial volume regulation. Arrows indicate currents in the presence of each compound. I_{ClSwell} was reduced by three well-known Cl⁻ channel blockers with diverse chemical structures (150 μ M NPPB, 300 μ M FFA and 500 μ M IAA-94) and, surprisingly, by the K⁺-Cl⁻ cotransport inhibitor DIOA (40 μ M). The current was not affected by either the Na⁺-K⁺-Cl⁻ cotransport inhibitor bumetanide (10 μ M) or the I_{ClIn} inhibitor acyclovir (100 μ M). (B) Isotonic volume regulation at room temperature. Ten minutes after applying each of the compounds in panel A to microglia in the isotonic bath solution, their volume (mean \pm SD) was measured and normalized to drug-free controls. The hatched bars indicate classical Cl⁻ channel blockers. Statistical differences from the controls were assessed by a one-way ANOVA, followed by Tukey's test ($*P < 0.05$) for the number of replicates indicated on each bar.

(Fig. 5A). Essentially complete inhibition is predicted for I_{ClIn} by acyclovir (Furst *et al.*, 2000), the K⁺-Cl⁻ cotransporter by DIOA, and the Na⁺-K⁺-Cl⁻ symporter by bumetanide (Taouil & Hannaert, 1999), but block of I_{ClSwell} was not anticipated. As expected, I_{ClSwell} was not

affected by 100 μM acyclovir ($4 \pm 5\%$, $n = 4$) or 10 μM bumetanide ($-9 \pm 11\%$, $n = 3$) but, surprisingly, 40 μM DIOA inhibited the current by $35 \pm 9\%$ (SD; $n = 3$). A similar DIOA concentration blocked an I_{Clswell} in nonpigmented ciliary epithelial cells (Botchkina & Matthews, 1995).

Before conducting RVD experiments, we used flow cytometry (see Materials and methods) to examine the normal volume of microglia suspended in an isotonic solution, and made a surprising observation: all compounds that reduced the current (IAA-94, NPPB, FFA and DIOA) significantly increased the baseline cell volume (measured 10 min after drug addition; Fig. 5B). Conversely, the compounds that did not affect the current (acyclovir and bumetanide) had no effect on homeostatic cell volume. RVD is usually considered the primary function of I_{Clswell} , and is recorded as cell swelling in hypotonic solution followed by a spontaneous return toward the initial volume. When transferred to 55% hypotonic solution, microglia swelled within 5 min to $\sim 155\%$ of their original volume at room temperature, and $\sim 140\%$ at 37 $^{\circ}\text{C}$ (Fig. 6A). RVD was slow and incomplete at both temperatures, with $\sim 26\%$ recovery by 30 min after the hypotonic shock at room temperature. Again, the drugs that reduced I_{Clswell} inhibited volume recovery (IAA-94, NPPB, FFA and DIOA), while acyclovir and bumetanide had no effect (Fig. 6B). FFA reduced RVD by $\sim 50\%$ but did not reach statistical significance based on the four experiments.

I_{Clswell} contributed to phagocytosis

Phagocytosis is an important function of microglia and involves dramatic shape changes, probably accompanied by volume changes. Thus, given the role of I_{Clswell} in both homeostatic volume regulation and RVD, one might anticipate a role in phagocytosis. The two most effective I_{Clswell} blockers (NPPB and FFA) were tested while monitoring phagocytosis of fluorescent-labelled *E. coli* for 1 h at 37 $^{\circ}\text{C}$. After quenching the fluorescence of any adhering *E. coli* (see Materials and methods), internalized bacteria were seen in most microglia (Fig. 7A). The assay was then conducted in multiwell plates, and showed that both I_{Clswell} blockers inhibited phagocytosis in a dose-dependent manner. The IC_{50} values were 13 μM for NPPB and 31 μM for FFA (Fig. 7B). These values compare quite well with the IC_{50} values we previously measured for I_{Clswell} block in microglia ($\sim 30 \mu\text{M}$ for NPPB and $\sim 80 \mu\text{M}$ for FFA; Schlichter *et al.*, 1996) and the concentrations needed to block the similar Cl^- current in T lymphocytes (Schumacher *et al.*, 1995), and argue for a specific role of I_{Clswell} in microglial phagocytosis.

Discussion

Comparison with I_{Clswell} in other cells

Table 2 summarizes several salient features of I_{Clswell} in rat microglia and compares them with other cells (for recent reviews on I_{Clswell} , see Jentsch *et al.*, 2002; d'Anglemon de Tassigny *et al.*, 2003; Nilius *et al.*, 2003; Sardini *et al.*, 2003). The microglial current is similar in having time- and voltage-independent activation, a halide ion selectivity sequence of $\Gamma^- = \text{Br}^- > \text{Cl}^- > \text{F}^-$, and sensitivity to the blockers NPPB and FFA. Some I_{Clswell} can be activated by reduced intracellular ionic strength without cell swelling (Nilius *et al.*, 1998), and this was true for the microglial current. Differences in pharmacology include poor block of the microglial current by SITS or DIDS (and no block by up to 10 mM external ATP; our unpublished observations). Biophysical differences include lack of inactivation and a smaller single-channel conductance. Most I_{Clswell} exhibit

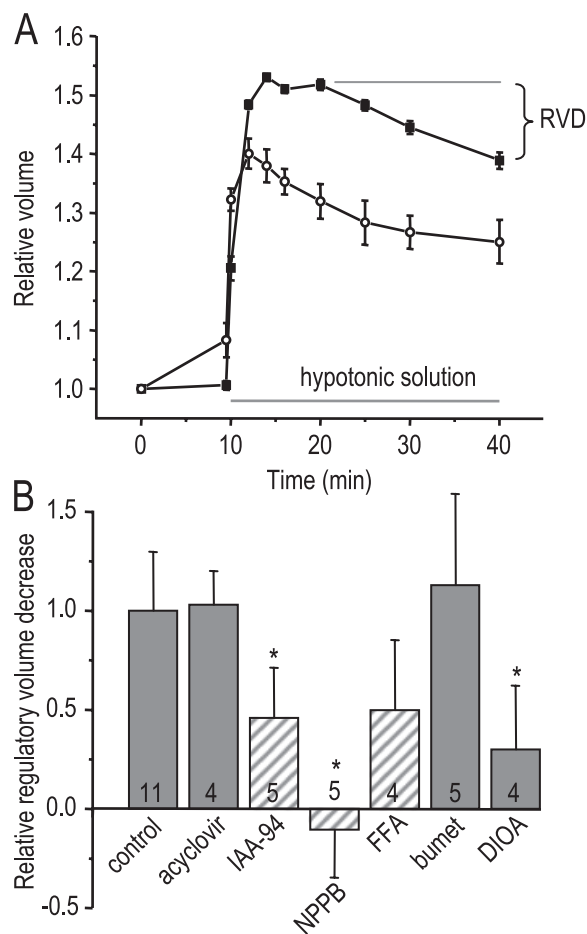


FIG. 6. Blockers of I_{Clswell} inhibited the RVD. (A) Summary of the time course of cell swelling and spontaneous volume recovery after applying a 55% hypotonic solution at room temperature (\blacksquare) or at 37 $^{\circ}\text{C}$ (\circ). Values were normalized to the resting volume in isotonic solution and plotted as mean \pm SD. (B) Effects of the compounds used in Fig. 5 on microglial RVD measured at room temperature. For each treatment, RVD was calculated as the difference in the relative volume at 5 min vs. 30 min after applying the hypotonic solution. The results were then normalized to drug-free control cells and plotted as mean \pm SD. The hatched bars indicate classical Cl^- channel blockers. Statistical differences from controls were assessed by a one-way ANOVA, followed by Tukey's tests ($*P < 0.05$) for the number of replicates indicated on each bar.

voltage-sensitive inactivation (Jackson & Strange, 1995a; Nilius *et al.*, 2003), although the rate and degree vary (Jentsch *et al.*, 2002), and may depend on extracellular Mg^{2+} (Braun & Schulman, 1996; Voets *et al.*, 1997). Microglia lack inactivation, even at strongly depolarized potentials, and with the highest divalent cation concentration used in previous I_{Clswell} studies. To help identify the underlying channel, the single-channel conductance is often calculated from noise analysis of whole-cell currents; however, some studies found that the critical assumption that I_{Clswell} activation is due to a graded increase in P_o was violated (Jackson *et al.*, 1995b; Boese *et al.*, 1996). From the differences in single-channel conductance based on stationary noise analysis during run-up (< 1 pS) and nonstationary analysis during inactivation (15 pS at 0 mV), it was concluded that current activation was due to a graded increase in the number of active channels, not in P_o (Jackson *et al.*, 1995b). Outward rectification and similar values (15–40 pS) have been observed from single-channel studies in myocytes and epithelial cells (Meyer & Korbacher, 1996; Wang *et al.*, 2005). As the microglial I_{Clswell} does not inactivate, we

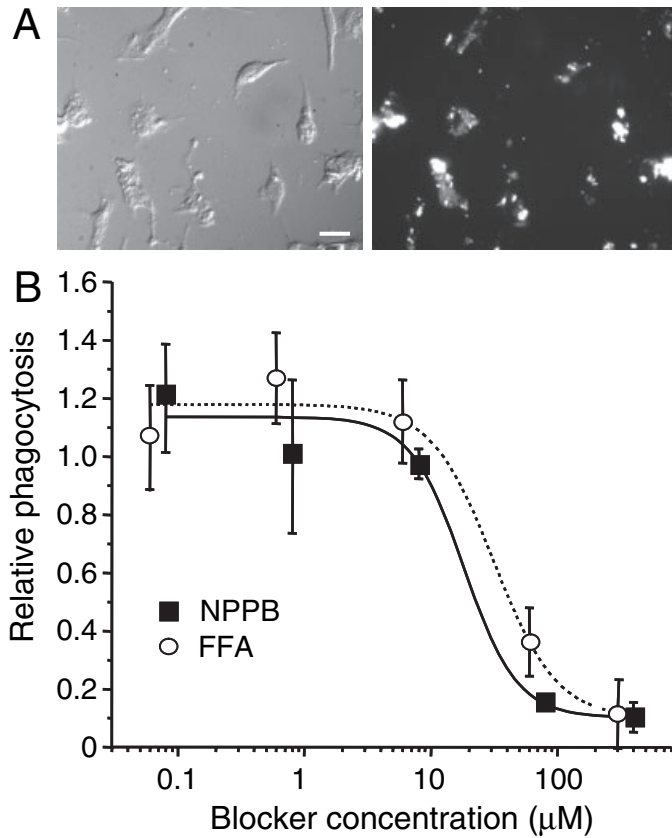


FIG. 7. $I_{Cl_{swell}}$ blockers inhibited phagocytosis. (A) Micrographs of microglia after exposure to fluorescent-labelled *E. coli*. Left, DIC image; right, fluorescence image of same field showing phagocytosed bacteria. (B) The Cl⁻ channel blockers FFA and NPPB inhibited phagocytosis in a dose-dependent manner. Phagocytosis at different blocker concentrations was normalized to the DMSO control, and each point is the average of three replicates (mean \pm SD). From fits to sigmoidal functions, the IC_{50} values for inhibiting phagocytosis were 31 μ M for FFA and 18 μ M for NPPB. Scale bar, 25 μ m.

compared mean-*vs*-variance analysis with a new approach wherein P_o was decreased by increasing the SITS concentration; both methods yielded a small conductance (\sim 1 and 3 pS). Overall, $I_{Cl_{swell}}$ in microglia most resembles a current in human lymphocytes which has the same selectivity sequence, a small single-channel conductance and a similar pharmacological profile, which lacks inactivation and which can be activated by low ionic strength (Lewis *et al.*, 1993; Schumacher *et al.*, 1995).

Molecular candidates for the microglia swelling-activated channel

The identity of $I_{Cl_{swell}}$ has long been debated, and it is often assumed that VRACs are the same gene product. However, the microglial $I_{Cl_{swell}}$ appears to be a different entity based on differences in inactivation, single-channel conductance and pharmacology. It is thus valuable to compare the properties of the several candidate genes expressed in rat microglia. $pI_{Cl_{in}}$ is no longer considered a candidate (Jentsch *et al.*, 2002; d'Anglemont de Tassigny *et al.*, 2003), although it might regulate $I_{Cl_{swell}}$ (Chen *et al.*, 1999). We ruled out a contribution of $I_{Cl_{in}}$ to the microglial current and volume regulation, as they were not affected by the $I_{Cl_{in}}$ inhibitor acyclovir (Furst *et al.*, 2000). CIC-2 is a small-conductance channel (\sim 2 pS; Weinreich & Jentsch, 2001) like the microglial $I_{Cl_{swell}}$, and is activated by cell

swelling (Grunder *et al.*, 1992), but differs in having a Cl⁻ > Br⁻ > I⁻ permeability sequence and hyperpolarization-induced activation (Thiemann *et al.*, 1992; Nilius *et al.*, 2003). The properties of CIC-3 have been very difficult to determine as it is ubiquitously expressed, but it has been proposed that CIC-3 produces a highly outward-rectified current, with a Cl⁻ > Br⁻ > I⁻ permeability sequence (Li *et al.*, 2000; Jentsch *et al.*, 2002), which is inconsistent with the microglial VRAC. Although it has been proposed that CIC-3 is a VRAC displaying inactivation and intermediate conductance (Duan *et al.*, 1997; Wang *et al.*, 2003), its properties, membrane expression and roles have been extensively debated (e.g. Li *et al.*, 2000; Stobrawa *et al.*, 2001; Nilius *et al.*, 2003; Wang *et al.*, 2005).

The contribution of the chloride intracellular channel (CLIC) family is controversial. Some investigators have proposed that soluble cytoplasmic CLIC1 molecules move into the plasma membrane (Tulk *et al.*, 2000; reviewed in Ashley, 2003), while others doubt that it is a Cl⁻ channel (Hartzell *et al.*, 2005). Based on heterologous expression of CLIC1, its biophysical properties are also controversial, with a reported single-channel conductance from 6 to 160 pS, and selectivity sequences of F⁻ > Cl⁻ > I⁻ or Br⁻ \approx Cl⁻ > I⁻ (reviewed in Ashley, 2003). Recently, CLIC1 was reported to form a small-conductance (6–7 pS) plasma membrane channel in rat microglia and the BV2 microglial cell line (Novarino *et al.*, 2004). Although we observed higher expression of CLIC1 mRNA than the other Cl⁻ channel genes examined, three observations argue against it encoding the microglial $I_{Cl_{swell}}$. First, single channels attributed to CLIC1 were seen in cell-attached recordings from microglia but no current was seen in whole-cell recordings (Novarino *et al.*, 2004), whereas we found that $I_{Cl_{swell}}$ could be activated by cell swelling for many minutes after going whole-cell. Second, the current from cloned CLIC1 is blocked by \leq 10 μ M IAA-94 (Valenzuela *et al.*, 2000; reviewed in Ashley, 2003), while 500 μ M produced only \sim 70% block in the present study. Third, the limited information on the permeability sequence of cloned CLIC1 (reviewed in Ashley, 2003) is clearly at odds with our results.

We believe that the best candidate for the microglial $I_{Cl_{swell}}$ lies within the recently discovered bestrophin gene family (reviewed in Hartzell *et al.*, 2005). Transcripts for Best1, 2, 3 and 4 were found in rat microglia and, although their properties have not been well characterized, several features are apparently similar to the microglial current. Similarities to the microglial current include: (i) hBest1 and mBest2 produce volume-sensitive Cl⁻ currents with no voltage-dependent inactivation (reviewed in Fischmeister & Hartzell, 2005; Hartzell *et al.*, 2005); (ii) two *Xenopus* bestrophins have a permeability sequence of I⁻ > Br⁻ > Cl⁻ (Qu *et al.*, 2003; Pifferi *et al.*, 2006); (iii) the *Drosophila* gene, dBest1, has a conductance of 2 pS (Chien *et al.*, 2006); and (iv) bestrophins are sensitive to high concentrations of SITS (complete block at 2 mM) and DIDS (\sim 50% block at 500 μ M; Sun *et al.*, 2002; Pifferi *et al.*, 2006). One possible difference is the reported sensitivity of some cloned bestrophins to intracellular Ca²⁺ however, it is unclear whether any or all bestrophins require elevated Ca²⁺. Before attempting to use siRNA-mediated knockdown to help identify the channel, more information is needed about the biophysical and pharmacological properties of the cloned channels in mammalian cells. In addition, we have found that siRNA-mediated knockdown is extremely inefficient in primary microglia. That is, despite testing many methods (> 15 different transfection reagents, several retroviral and lentiviral constructs, electroporation and AmaxaTM nucleofection), none yielded effective transfection or infection, and most treatments damaged the microglia.

TABLE 2. Comparison of salient properties of $I_{Clswell}$ in microglia and other cells

Microglia	Comments and comparisons
Voltage dependence Rectification: mildly outward rectifying ^{1,2,3} Activation: not time- or V_m -dependent ^{1,2,3} Activated by low internal ionic strength without swelling ¹ Inactivation: none ^{1,2} , even at +100 mV, with or without high Mg^{2+} ¹	Many $I_{Clswell}$ are more outwardly rectifying ⁶⁻⁹ microglia are similar to T lymphocytes ^{10, 11} Similar to most $I_{Clswell}$ ⁶⁻⁹ Similar to some $I_{Clswell}$ ¹² Variable; some increased by high Mg^{2+} ^{13,14} microglia are similar to T lymphocytes ^{10, 11}
Single-channel conductance During run-up: 0.72 ± 0.17 pS ¹ During SITS block: 3.54 ± 1.31 pS ¹	Some $I_{Clswell}$ are outward rectifying ($\sim 15-40$ pS): during inactivation ^{4,5} or from single-channel recordings ^{15,16} Not tested on other $I_{Clswell}$
Permeability sequence $\Gamma \geq Br^- > Cl^- > F^- > aspartate \geq glutamate$ ^{1,11}	Eisenman sequence I (for halides); similar to many $I_{Clswell}$ ⁶⁻⁹
Channel blockers ATP _o NPPB, $IC_{50} \sim 30$ μM IAA-94, $IC_{50} \sim 200$ μM ² FFA, $IC_{50} \sim 80$ μM ² DIDS, $IC_{50} = 16.1$ μM at +40 mV ³ SITS, $IC_{50} = 71$ μM at +40 mV ³ DIAO (35 \pm 9% block at 40 μM) ¹	ATP _o blocks many $I_{Clswell}$ ⁶⁻⁹ but not microglia NPPB blocks many $I_{Clswell}$ ⁶⁻⁹ FFA blocks many $I_{Clswell}$ ⁶⁻⁹ V_m -dependent block ^{1,2} ; higher IC_{50} expected at -ve V_{rest} Most $I_{Clswell}$ are more sensitive ⁶⁻⁹ Not tested on other $I_{Clswell}$
Volume regulation: volume vs. control, isotonic¹ and RVD^{1,2} (isotonic volume regulation not tested	for other $I_{Clswell}$)
Acyclovir (100 μM) IAA-94 (500 μM) NPPB (150 μM) FFA (300 μM) Bumetanide (10 μM) DIOA (40 μM)	1.00 (isotonic) and 1.03 (RVD) 1.10 (isotonic) and 0.46 (RVD) 1.15 (isotonic) and -0.10* (RVD) 1.10 (isotonic) and 0.50 (RVD) 1.00 (isotonic) and 1.13 (RVD) 1.10 (isotonic) and 0.30 (RVD)
Inhibition of phagocytosis (role in phagocytosis not tested for other $I_{Clswell}$) NPPB, $IC_{50} = 13$ μM FFA, $IC_{50} = 31$ μM	

References: ¹present study; ²Schlichter *et al.* (1996); ³Eder *et al.* (1998); ⁴Jackson *et al.* (1995b); ⁵Boese *et al.* (1996); ⁶Jentsch *et al.* (2002); ⁷d'Anglemont de Tassigny *et al.* (2003); ⁸Nilius *et al.* (2003); ⁹Sardini *et al.* (2003); ¹⁰Lewis *et al.* (1993); ¹¹Schumacher *et al.* (1995); ¹²Nilius *et al.* (1998); ¹³Braun *et al.* (1996); ¹⁴Voets *et al.* (1997); ¹⁵Meyer *et al.* (1996); ¹⁶Wang *et al.* (2005). *The negative sign (-0.10) indicates an increase in volume.

Roles of Cl^- channels in microglia functions

Given the numerous candidate genes in rat microglia and the relatively poor pharmacological tools available (e.g. compared with K^+ channel blockers), it has been difficult to ascribe a specific physiological function to a cloned Cl^- channel. $I_{Clswell}$ (Schlichter *et al.*, 1996; present study) and a stretch-sensitive Cl^- channel in microglia (Eder *et al.*, 1998) have similar outward rectification, voltage-independent activation, lack of inactivation, and pharmacological profile; thus, we speculate that they are both mediated the same member of the bestrophin family. In contrast, little is known about a chemokine-induced Cl^- current (Rappert *et al.*, 2002) and, as explained above, the CLIC1-like channels (Novarino *et al.*, 2004) are very likely a different gene product.

The present study adds important information about the roles of Cl^- channels in microglia. The most widely studied role of Cl^- channels in immune cells is the RVD that follows cell swelling. Our results support a role in RVD but also provide the first evidence that the current is involved in homeostatic volume regulation. Both forms of volume regulation were affected by the same three blockers of $I_{Clswell}$ (NPPB, FFA and IAA-94) and, surprisingly, by the K^+-Cl^- cotransport inhibitor DIOA, which we found also inhibits $I_{Clswell}$. The latter finding raises questions about studies that use DIOA to invoke a role for K^+-Cl^- cotransport in microglia (e.g. Schilling *et al.*, 2004). [The pharmacology argues against involvement of I_{Cl} (no effect of acyclovir) or the $Na^+-K^+-Cl^-$ symporter (no effect of bumetanide).] The effect of Cl^- channel blockade on the resting microglia volume implies that some Cl^-

channels are active under resting conditions. This contention is supported by our earlier finding that Cl^- channels strongly regulate the microglial membrane potential and that, owing to the very high membrane resistance, a small Cl^- current is sufficient (Newell *et al.*, 2005). A role for $I_{Clswell}$ in homeostatic volume regulation might also account for the ability of FFA and NPPB to inhibit morphological changes in murine microglia (Eder *et al.*, 1998). Phagocytosis by microglia is an essential function both in developmental refinement of the healthy CNS and for removing invading organisms and damaged cells and debris in the damaged CNS. Very little is known about involvement of ion channels in phagocytosis. Acidification of the phagosome involves the Cl^- channel, CFTR, but phagocytosis is not affected in *Cftr*-null mice (Di *et al.*, 2006). *CIC-3*-knockout mice showed defective phagocytosis by neutrophils and, because *CIC-3* is a vesicular protein, its mechanism was thought to be through intracellular signalling (Moreland *et al.*, 2006). Here, the inhibition of phagocytosis of *E. coli* particles and $I_{Clswell}$ by similar concentrations of FFA and NPPB provides the first evidence for involvement of an $I_{Clswell}$ in phagocytosis, but the lack of highly selective blockers means we cannot rule out other Cl^- channels. Nevertheless, the apparent involvement of $I_{Clswell}$ in volume regulation and phagocytosis raises the intriguing possibility that these roles are linked because phagocytosis is accompanied by dramatic shape changes and an increase in cell volume (Bos & de Souza, 2001), especially as osmolyte efflux might compensate for phagocytosis-induced volume increases (Warskulat *et al.*, 1996). This hypothesis is also consistent with inhibition of phagocytosis by Kupffer cells (liver macrophages)

and a mouse macrophage cell line by hyperosmotic solutions (Warskulat *et al.*, 1996), and inhibition by classical Cl⁻ channel blockers of release of osmolytes during phagocytosis (Wettstein *et al.*, 2000).

Acknowledgements

We are grateful to Xiaoping Zhu for excellent technical assistance. Funded by operating grants to LCS from the Canadian Institutes of Health Research (MT-13657) and the Heart & Stroke Foundation, Ontario chapter (T4670; T5782). E.W.N. was supported by a National Institutes of Health (USA), Kirschstein Predoctoral National Research Service Award (no. F31NS049742).

Abbreviations

CLIC, chloride intracellular channel; DIDS, 4,4'-diisothiocyanatostilbene-2,2'-disulphonic acid; DIOA, [(dihydroindenyl)oxy]acetic acid; FFA, flufenamic acid; HPRT-1, hypoxanthine guanine phosphoribosyl transferase; IAA-94, indanylalkanoic acid; I_{Cl,swell}, swelling-activated Cl⁻ current; NMDG⁺, N-methyl-D-glucamine; NPPB, 5-nitro-2-(3-phenylpropylamino) benzoic acid; qRT-PCR, quantitative real-time reverse transcriptase-polymerase chain reaction; RVD, regulatory volume decrease; SITS, 4-acetamido-4'-isothiocyanatostilbene-2,2'-disulphonic acid; VRAC, volume-regulated anion channel.

References

d'Anglemont de Tassigny, A., Souktani, R., Ghaleh, B., Henry, P. & Berdeaux, A. (2003) Structure and pharmacology of swelling-sensitive chloride channels, I_{Cl,swell}. *Fundam. Clin. Pharmacol.*, **17**, 539–553.

Ashley, R.H. (2003) Challenging accepted ion channel biology: p64 and the CLIC family of putative intracellular anion channel proteins (Review). *Mol. Membr. Biol.*, **20**, 1–11.

Boese, S.H., Kinne, R.K. & Wehner, F. (1996) Single-channel properties of swelling-activated anion conductance in rat inner medullary collecting duct cells. *Am. J. Physiol.*, **271**, F1224–F1233.

Bos, H. & de Souza, W. (2001) Morphometrical method for estimating mean cell volume of phagocytosing cells. *Microsc. Microanal.*, **7**, 39–47.

Botchkina, L.M. & Matthews, G. (1995) Swelling activates chloride current and increases internal calcium in nonpigmented epithelial cells from the rabbit ciliary body. *J. Cell Physiol.*, **164**, 286–294.

Braun, A.P. & Schulman, H. (1996) Distinct voltage-dependent gating behaviours of a swelling-activated chloride current in human epithelial cells. *J. Physiol. (Lond.)*, **495**, 743–753.

Bustin, S.A. & Nolan, T. (2004) Pitfalls of quantitative real-time reverse-transcription polymerase chain reaction. *J. Biomol. Technol.*, **15**, 155–166.

Chen, L., Wang, L. & Jacob, T.J. (1999) Association of intrinsic pCl_{in} with volume-activated Cl⁻ current and volume regulation in a native epithelial cell. *Am. J. Physiol.*, **276**, C182–C192.

Chien, L.T., Zhang, Z.R. & Hartzell, H.C. (2006) Single Cl⁻ channels activated by Ca²⁺ in *Drosophila* S2 cells are mediated by bestrophins. *J. General Physiol.*, **128**, 247–259.

Di, A., Brown, M.E., Deriy, L.V., Li, C., Szeto, F.L., Chen, Y., Huang, P., Tong, J., Naren, A.P., Bindokas, V., Palfrey, H.C. & Nelson, D.J. (2006) CFTR regulates phagosome acidification in macrophages and alters bactericidal activity. *Nat. Cell Biol.*, **8**, 933–944.

Downey, G.P., Grinstein, S., Sue, A.Q., Czaban, B. & Chan, C.K. (1995) Volume regulation in leukocytes: requirement for an intact cytoskeleton. *J. Cell Physiol.*, **163**, 96–104.

Duan, D., Winter, C., Cowley, S., Hume, J.R. & Horowitz, B. (1997) Molecular identification of a volume-regulated chloride channel. *Nature*, **390**, 417–421.

Eder, C., Klee, R. & Heinemann, U. (1998) Involvement of stretch-activated Cl⁻ channels in ramification of murine microglia. *J. Neurosci.*, **18**, 7127–7137.

Fischmeister, R. & Hartzell, H.C. (2005) Volume sensitivity of the bestrophin family of chloride channels. *J. Physiol. (Lond.)*, **562**, 477–491.

Fordyce, C.B., Jagasia, R., Zhu, X. & Schlichter, L.C. (2005) Microglia Kv1.3 channels contribute to their ability to kill neurons. *J. Neurosci.*, **25**, 7139–7149.

Furst, J., Bazzini, C., Jakab, M., Meyer, G., Konig, M., Gschwentner, M., Ritter, M., Schmarda, A., Botta, G., Benz, R., Deetjen, P. & Paulmichl, M. (2000) Functional reconstitution of ICln in lipid bilayers. *Pflugers Arch.*, **440**, 100–115.

Grunder, S., Thiemann, A., Pusch, M. & Jentsch, T.J. (1992) Regions involved in the opening of CIC-2 chloride channel by voltage and cell volume. *Nature*, **360**, 759–762.

Hartzell, C., Qu, Z., Putzier, I., Artinian, L., Chien, L.T. & Cui, Y. (2005) Looking chloride channels straight in the eye: bestrophins, lipofuscinosis, and retinal degeneration. *Physiology (Bethesda)*, **20**, 292–302.

Jackson, P.S. & Strange, K. (1995a) Characterization of the voltage-dependent properties of a volume-sensitive anion conductance. *J. General Physiol.*, **105**, 661–676.

Jackson, P.S. & Strange, K. (1995b) Single-channel properties of a volume-sensitive anion conductance. Current activation occurs by abrupt switching of closed channels to an open state. *J. General Physiol.*, **105**, 643–660.

Jentsch, T.J., Stein, V., Weinreich, F. & Zdebik, A.A. (2002) Molecular structure and physiological function of chloride channels. *Physiol. Rev.*, **82**, 503–568.

Kaushal, V., Koeberle, P.D., Wang, Y. & Schlichter, L.C. (2007) The Ca²⁺-activated K⁺ channel KCNN4/KCa3.1 contributes to microglia activation and nitric oxide-dependent neurodegeneration. *J. Neurosci.*, **27**, 234–244.

Khanna, R., Chang, M.C., Joiner, W.J., Kaczmarek, L.K. & Schlichter, L.C. (1999) hSK4/hIK1, a calmodulin-binding KCa channel in human T lymphocytes. Roles in proliferation and volume regulation. *J. Biol. Chem.*, **274**, 14838–14849.

Kim, M.J., Cheng, G. & Agrawal, D.K. (2004) Cl⁻ channels are expressed in human normal monocytes: a functional role in migration, adhesion and volume change. *Clin. Exp. Immunol.*, **138**, 453–459.

Lewis, R.S., Ross, P.E. & Cahalan, M.D. (1993) Chloride channels activated by osmotic stress in T lymphocytes. *J. General Physiol.*, **101**, 801–826.

Li, X., Shimada, K., Showalter, L.A. & Weinman, S.A. (2000) Biophysical properties of CIC-3 differentiate it from swelling-activated chloride channels in Chinese hamster ovary-K1 cells. *J. Biol. Chem.*, **275**, 35994–35998.

Meyer, K. & Korbmacher, C. (1996) Cell swelling activates ATP-dependent voltage-gated chloride channels in M-1 mouse cortical collecting duct cells. *J. General Physiol.*, **108**, 177–193.

Mignen, O., Le, G.C., Harvey, B.J. & Thomas, S. (1999) Volume regulation following hypotonic shock in isolated crypts of mouse distal colon. *J. Physiol. (Lond.)*, **515**, 501–510.

Moreland, J.G., Davis, A.P., Bailey, G., Nauseef, W.M. & Lamb, F.S. (2006) Anion channels, including CIC-3, are required for normal neutrophil oxidative function, phagocytosis, and transendothelial migration. *J. Biol. Chem.*, **281**, 12277–12288.

Newell, E.W. & Schlichter, L.C. (2005) Integration of K⁺ and Cl⁻ currents regulate steady-state and dynamic membrane potentials in cultured rat microglia. *J. Physiol. (Lond.)*, **567**, 869–890.

Nilius, B. & Droogmans, G. (2003) Amazing chloride channels: an overview. *Acta Physiol. Scand.*, **177**, 119–147.

Nilius, B., Prenen, J., Voets, T., Eggermont, J. & Droogmans, G. (1998) Activation of volume-regulated chloride currents by reduction of intracellular ionic strength in bovine endothelial cells. *J. Physiol. (Lond.)*, **506**, 353–361.

Novarino, G., Fabrizi, C., Tonini, R., Denti, M.A., Malchiodi-Albedi, F., Lauro, G.M., Sacchetti, B., Paradisi, S., Ferroni, A., Curmi, P.M., Breit, S.N. & Mazzanti, M. (2004) Involvement of the intracellular ion channel CLIC1 in microglia-mediated beta-amyloid-induced neurotoxicity. *J. Neurosci.*, **24**, 5322–5330.

Okada, Y., Shimizu, T., Maeno, E., Tanabe, S., Wang, X. & Takahashi, N. (2006) Volume-sensitive chloride channels involved in apoptotic volume decrease and cell death. *J. Membr. Biol.*, **209**, 21–29.

Ormerod, M.G., Paul, F., Cheetham, M. & Sun, X.M. (1995) Discrimination of apoptotic thymocytes by forward light scatter. *Cytometry*, **21**, 300–304.

Pahapill, P.A. & Schlichter, L.C. (1992) Modulation of potassium channels in intact human T lymphocytes. *J. Physiol. (Lond.)*, **445**, 407–430.

Pifferi, S., Pascarella, G., Boccaccio, A., Mazzatenta, A., Gustincich, S., Menini, A. & Zucchelli, S. (2006) Bestrophin-2 is a candidate calcium-activated chloride channel involved in olfactory transduction. *Proc. Natl. Acad. Sci. USA*, **103**, 12929–12934.

Qu, Z., Wei, R.W., Mann, W. & Hartzell, H.C. (2003) Two bestrophins cloned from *Xenopus laevis* oocytes express Ca²⁺-activated Cl⁻ currents. *J. Biol. Chem.*, **278**, 49563–49572.

Ransom, C.B., O'Neal, J.T. & Sontheimer, H. (2001) Volume-activated chloride currents contribute to the resting conductance and invasive migration of human glioma cells. *J. Neurosci.*, **21**, 7674–7683.

- Rappert, A., Biber, K., Nolte, C., Lipp, M., Schubel, A., Lu, B., Gerard, N.P., Gerard, C., Boddeke, H.W. & Kettenmann, H. (2002) Secondary lymphoid tissue chemokine (CCL21) activates CXCR3 to trigger a Cl^- current and chemotaxis in murine microglia. *J. Immunol.*, **168**, 3221–3226.
- Roman, R.M., Wang, Y. & Fitz, J.G. (1996) Regulation of cell volume in a human biliary cell line: activation of K^+ and Cl^- currents. *Am. J. Physiol.*, **271**, G239–G248.
- Sardini, A., Amey, J.S., Weylandt, K.H., Nobles, M., Valverde, M.A. & Higgins, C.F. (2003) Cell volume regulation and swelling-activated chloride channels. *Biochim. Biophys. Acta*, **1618**, 153–162.
- Schilling, T., Lehmann, F., Ruckert, B. & Eder, C. (2004) Physiological mechanisms of lysophosphatidylcholine-induced de-ramification of murine microglia. *J. Physiol. (Lond.)*, **557**, 105–120.
- Schlichter, L.C., Sakellaropoulos, G., Ballyk, B., Pennefather, P.S. & Phipps, D.J. (1996) Properties of K^+ and Cl^- channels and their involvement in proliferation of rat microglial cells. *Glia*, **17**, 225–236.
- Schumacher, P.A., Sakellaropoulos, G., Phipps, D.J. & Schlichter, L.C. (1995) Small-conductance chloride channels in human peripheral T lymphocytes. *J. Membr. Biol.*, **145**, 217–232.
- Shen, M.R., Droogmans, G., Eggermont, J., Voets, T., Ellory, J.C. & Nilius, B. (2000) Differential expression of volume-regulated anion channels during cell cycle progression of human cervical cancer cells. *J. Physiol. (Lond.)*, **529**, 385–394.
- Stobrawa, S.M., Breiderhoff, T., Takamori, S., Engel, D., Schweizer, M., Zdebik, A.A., Bosl, M.R., Ruether, K., Jahn, H., Draguhn, A., Jahn, R. & Jentsch, T.J. (2001) Disruption of ClC-3 , a chloride channel expressed on synaptic vesicles, leads to a loss of the hippocampus. *Neuron*, **29**, 185–196.
- Sun, H., Tsunenari, T., Yau, K.W. & Nathans, J. (2002) The vitelliform macular dystrophy protein defines a new family of chloride channels. *Proc. Natl. Acad. Sci. USA*, **99**, 4008–4013.
- Taouil, K. & Hannaert, P. (1999) Evidence for the involvement of K^+ channels and K^+ - Cl^- cotransport in the regulatory volume decrease of newborn rat cardiomyocytes. *Pflugers Arch.*, **439**, 56–66.
- Thiemann, A., Grunder, S., Pusch, M. & Jentsch, T.J. (1992) A chloride channel widely expressed in epithelial and non-epithelial cells. *Nature*, **356**, 57–60.
- Tulk, B.M., Schlesinger, P.H., Kapadia, S.A. & Edwards, J.C. (2000) CLIC-1 functions as a chloride channel when expressed and purified from bacteria. *J. Biol. Chem.*, **275**, 26986–26993.
- Valenzuela, S.M., Mazzanti, M., Tonini, R., Qiu, M.R., Warton, K., Musgrove, E.A., Campbell, T.J. & Breit, S.N. (2000) The nuclear chloride ion channel NCC27 is involved in regulation of the cell cycle. *J. Physiol. (Lond.)*, **529**, 541–552.
- Voets, T., Droogmans, G. & Nilius, B. (1997) Modulation of voltage-dependent properties of a swelling-activated Cl^- current. *J. General Physiol.*, **110**, 313–325.
- Wang, G.X., Hatton, W.J., Wang, G.L., Zhong, J., Yamboliev, I., Duan, D. & Hume, J.R. (2003) Functional effects of novel anti- ClC-3 antibodies on native volume-sensitive osmolyte and anion channels in cardiac and smooth muscle cells. *Am. J. Physiol. Heart Circ. Physiol.*, **285**, H1453–H1463.
- Wang, J., Xu, H., Morishima, S., Tanabe, S., Jishage, K., Uchida, S., Sasaki, S., Okada, Y. & Shimizu, T. (2005) Single-channel properties of volume-sensitive Cl^- channel in ClC-3 -deficient cardiomyocytes. *Jpn. J. Physiol.*, **55**, 379–383.
- Warskulat, U., Zhang, F. & Haussinger, D. (1996) Modulation of phagocytosis by anisoosmolarity and betaine in rat liver macrophages (Kupffer cells) and RAW 264.7 mouse macrophages. *FEBS Lett.*, **391**, 287–292.
- Weinreich, F. & Jentsch, T.J. (2001) Pores formed by single subunits in mixed dimers of different ClC chloride channels. *J. Biol. Chem.*, **276**, 2347–2353.
- Wettstein, M., Peters-Regehr, T., Kubitz, R., Fischer, R., Holneicher, C., Monnighoff, I. & Haussinger, D. (2000) Release of osmolytes induced by phagocytosis and hormones in rat liver. *Am. J. Physiol. Gastrointest. Liver Physiol.*, **278**, G227–G233.
- Wundergem, R., Gong, W., Monen, S.H., Dooley, S.N., Gonce, J.L., Conner, T.D., Houser, M., Ecay, T.W. & Ferslew, K.E. (2001) Blocking swelling-activated chloride current inhibits mouse liver cell proliferation. *J. Physiol. (Lond.)*, **532**, 661–672.